Development 134, 2851-2861 (2007) doi:10.1242/dev.003517

# A novel eIF4G homolog, Off-schedule, couples translational control to meiosis and differentiation in *Drosophila* spermatocytes

**Tina M. Franklin-Dumont[1], Chandrima Chatterjee[1], Steven A. Wasserman[2] and Stephen DiNardo[1,*]**

During spermatogenesis, cells coordinate differentiation with the meiotic cell cycle to generate functional gametes. We identified a novel gene, which we named *off-schedule* (*ofs*), as being essential for this coordinated control. During the meiotic $G_2$ phase, *Drosophila ofs* mutant germ cells do not reach their proper size and fail to execute meiosis or significant differentiation. The accumulation of four cell cycle regulators – Cyclin A, Boule, Twine and Roughex – is altered in these mutants, indicating that *ofs* reveals a novel branch of the pathway controlling meiosis and differentiation. Ofs is homologous to eukaryotic translation initiation factor eIF4G. The level of *ofs* expression in spermatocytes is much higher than for the known eIF4G ortholog (known as eIF-4G or eIF4G), suggesting that Ofs substitutes for this protein. Consistent with this, assays for association with mRNA cap complexes, as well as RNA-interference and phenotypic-rescue experiments, demonstrate that Ofs has eIF4G activity. Based on these studies, we speculate that spermatocytes monitor $G_2$ growth as one means to coordinate the initiation of meiotic division and differentiation.

**KEY WORDS: Spermatogenesis, Meiosis, Cell cycle, Differentiation, Translation initiation, eIF4G, *Drosophila***

## INTRODUCTION

In spermatogenesis, progenitor cells must execute the meiotic divisions in coordination with acquiring the specialized morphology and functionality of sperm. This conserved process is particularly amenable to analysis in *Drosophila*. The fly testis is a blind-ended tube organized as an assembly line for spermatogenesis. Germline stem cells at the blind end give rise to gonialblasts, which divide mitotically four times with incomplete cytokinesis to produce a cyst of 16 interconnected spermatogonia. These cells exit the mitotic cycle and enter meiosis as spermatocytes, exhibiting an extended $G_2$ phase characterized by a significant increase in cell mass and robust transcription. At the end of $G_2$, the spermatocytes undergo the meiotic divisions and begin the conversion from round spermatids to specialized spermatozoa (Fuller, 1993).

Ten 'spermatocyte arrest' genes are required for both meiosis and differentiation and are sorted into two classes according to their molecular targets and specific role in promoting transcription (Ayyar et al., 2003; Hiller et al., 2004; Hiller et al., 2001; Jiang and White-Cooper, 2003; Lin et al., 1996; Perezgasga et al., 2004). The always early (aly) class affects the transcription of meiotic genes such *boule*, *twine* and *cyclin B*, as well as that of differentiation genes such as *fuzzy onions* (*fzo*) and *don juan* (White-Cooper et al., 1998). Notably, these mutations do not effect transcription of other spermatocyte genes, such as *pelota*, *cyclin A* and *roughex*. The Aly class proteins are thought to alter chromatin structure to permit the high levels of transcription necessary in spermatocytes (Ayyar et al., 2003; Jiang and White-Cooper, 2003; Perezgasga et al., 2004; White-Cooper et al., 2000). The cannonball (can) class affects *boule* and *twine* expression post-transcriptionally only and has no effect on *cyclin B*. The post-transcriptional effects must be indirect, because all *can* class loci encode testis-specific components of the general transcriptional machinery (Hiller et al., 2004; Hiller et al., 2001). Together, the spermatocyte arrest genes reveal how a diverse set of genes is selectively transcribed in spermatocytes.

The transcriptional regulatory pathway does not address the timing of meiotic entry and differentiation, however. Although transcripts necessary for these processes accumulate in early spermatocytes, the corresponding proteins do not appear until much later (White-Cooper et al., 1998). Because there is little, if any, transcription after the $G_2$-M transition in flies (Olivieri and Olivieri, 1965), spermatocytes must delay meiotic division until all the necessary transcripts have accumulated. A similar dilemma exists during the mitotic cycle in yeast. For cells to maintain the same average size over several divisions, control points act during the gap phases and allow cell cycle progression only when the cell has reached a threshold size, with $G_1$ predominating in budding yeast and $G_2$ in fission yeast (Rupes, 2002). Cell growth rates also feed back on mitotic cell cycle progression in *Drosophila* cells (Stocker and Hafen, 2000). Less is known about how growth might affect the specialized meiotic cell cycle.

Our identification and characterization of *off-schedule* (*ofs*) provides evidence that cell growth is linked to the coordination of meiosis and differentiation. Spermatocytes in *ofs* mutant males failed to execute the $G_2$-M transition of meiosis or substantive post-meiotic differentiation and had a significant cell size defect. The Off-schedule protein was found to resemble the eukaryotic initiation factor 4G (eIF4G), which is a member of the eIF4F translation initiation complex and bridges mature mRNAs and the ribosome (Prevot et al., 2003). The eIF4G activity of Ofs was apparent in its ability to associate with mRNA caps and to functionally replace canonical eIF4G (also known as eIF-4G – FlyBase) in cell culture. Because translation is primarily regulated at initiation, eIF4G is instrumental in determining the translational capacity of a cell and thus its ability to accumulate mass. Thus, the *ofs* mutant phenotype suggests that sufficient cell mass must accumulate before spermatocytes execute meiosis and differentiation.

[1]Department of Cell and Developmental Biology, University of Pennsylvania School of Medicine, Philadelphia, PA 19104-6048, USA. [2]Section of Cell and Developmental Biology, University of California, San Diego, La Jolla 92093, USA.

*Author for correspondence (e-mail: sdinardo@mail.med.upenn.edu)

**Accepted 2 June 2007**

## MATERIALS AND METHODS

### Fly stocks

Testes from males homozygous for a P element-generated deletion, *ofs*$^{3572D\text{-}175ca}$, contained few sperm tails. Complementation against EMS-induced male sterile mutants identified the second allele, *ofs*$^{Z3\text{-}3283}$ (Wakimoto et al., 2004). *rux*$^{9}$ (*roughex*$^{9}$) is a presumed null (Gönczy et al., 1994). Mosaic analysis with repressible cell marker (MARCM) clones were generated in *y w hsFLP Tub-GAL4 UAS-GFP:myc-nls; +; FRT82B ofs*$^{Z3\text{-}3283}$*/FRT82B Tub-GAL80* males [MARCM stocks from Ken Irvine (Rutgers, Piscataway, NJ) and Gary Struhl (Columbia University, New York, NY)] (Lee and Luo, 1999). Clones were induced in wandering third instar larvae, and flies were aged 1-3 days at 25°C and an additional 6 days at 29°C. For *lacZ*-marked clones, we used FRT82B ms(3)1011 (an insertion at *effete*, which results in *lacZ* expression throughout the male germline) (Castrillon et al., 1993). These clones were induced in pupae or newly eclosed adult males; flies were aged at 25°C. *twine-lacZ* has been described previously (White-Cooper et al., 1998).

### Microscopy

For phase microscopy of unfixed samples, testes were dissected in *Drosophila* ringers solution, placed in 15 μl on a slide and overlaid with a coverslip. BrdU pulse labeling was for 20-30 minutes at room temperature, as was previously described (Wallenfang et al., 2006). Frozen split squashes were as described in Li et al. (Li et al., 2004). β-galactosidase-activity stains on testes from newly eclosed males homozygous for the *twine-lacZ* insertion were as in Gönczy et al. (Gönczy et al., 1992). Immunofluorescence on whole mounts was as described in Terry et al. (Terry et al., 2006). Primary antibody incubations were overnight at 4°C unless noted: 1:50-100 mouse α-Cyclin A-A19, 1:1000 rabbit α-Boule (R383) (Cheng et al., 1998), 1:4000 rabbit α-Aly (White-Cooper et al., 1998), 1:700 rabbit α-Fzo (Hales and Fuller, 1997), 1:20 mouse α-Cyclin B-F2, 1:4000 rabbit α-lamin-Dm$_0$ (Smith and Fisher, 1989), 1:1000 rabbit α-GFP (1 hour, room temperature; Molecular Probes), 1:1000 rabbit α-Rux (Avedisov et al., 2000), 1:500 rabbit α-eIF4G (p180) (Zapata et al., 1994) and 1:10 mouse α-BrdU (90 minutes, 25°C; Becton-Dickinson). Images were captured using a Zeiss microscope with Apotome illumination.

### In situ hybridizations

Probes were synthesized from cDNAs AT30049 (*ofs*; Fig. 5A) and RE34257 (*eIF4G*) using the Dig RNA labeling kit (Roche Boehringer Mannheim), treated with DNase I, hydrolyzed in carbonate buffer and precipitated. Testes were fixed in 4% formaldehyde in PBS for 15 minutes on ice, then in 4% formaldehyde in PBS with 0.1% Tween-20 and 0.1% Na deoxycholate for 15 minutes at room temperature, treated with Proteinase K and fixed a third time in 4% formaldehyde in PBS with 0.1% Tween-20 for 30 minutes at room temperature. Hybridization was overnight at 65°C in 50% formamide, 5×SSC, 100 μg/ml salmon sperm DNA, 50 μg/ml heparin and 0.1% Tween-20, adjusted to pH 4.5 with citric acid. An α–Digoxygenin-AP secondary antibody (Roche) was used at 1:2000, either overnight at 4°C or for 1 hour at room temperature, and reactions were developed with NBT/BCIP.

### Cloning

The 3572D-175ca deletion was generated by male recombination using insertion EP(3)3572 (Preston and Engels, 1996). Complementation between 3572D-175ca and other deletions that we generated, including 3572D-197e (which complemented 3572D-175ca), defined a roughly 2 kb relevant region. This comprised the 5′ UTR for two nested genes, CG10192 and CG33111, and included 45 bases of the CG10192 coding region (Fig. 5A). CG10192 and CG33111 coding regions were then sequenced from *ofs*$^{Z3\text{-}3283}$ and two isogenic controls (Z3-0105 and Z3-5364). Only one base change was found: a C to T change (Gln798>Stop) in CG10192.

cDNA mapping and 5′ and 3′ RACE showed that CG10192 and CG33111 share an alternatively spliced 5′ UTR (Fig. 5A, transcripts A-D) but have distinct ORFs and 3′ UTRs. A 117 bp region encoding no recognizable protein domains is alternatively spliced out of the first exon of CG10192 (Fig. 5A,B). Reverse transcriptase (RT)-PCR analysis from testis RNA verified that this was the only alternative splicing in the CG10192 coding region. Details of transcript mapping are available upon request. The rescue construct contained 328 bp of 5′ UTR common to all splice variants, the full-length coding region and 298 bp of the 3′ UTR, assembled by RT-PCR and cloned into an hs83 promoter P element vector (Horabin and Schedl, 1993).

### Cell culture

We plated 4.5 million S2R+ cells in six-well plates in Insectagro (Mediatech) supplemented with 7.5% fetal bovine serum and penicillin/streptomycin. Transfections were carried out the following day (Effectene; Qiagen). For the cap-association experiments, cells were harvested 2 days post-transfection and lysed in 50 mM Tris-Cl (pH 7.5), 150 mM NaCl, 1% Tween-20, 0.3% Igepal with a protease inhibitor cocktail (Sigma), 1 mM NaF, 1 mM activated sodium orthovanadate and 1 mM PMSF on ice for 15 minutes. GTP (100 mM) and 1 mM DTT were added for 10 minutes on ice, and then lysates were incubated with pre-blocked 7-methyl-GTP Sepharose 4B or Glutathione Sepharose 4B (GE, Amersham) overnight at 4°C. Beads were washed twice in lysis buffer then in PBS and resuspended in 1×SDS-PAGE sample buffer, boiled and analyzed by western blot.

dsRNA target regions were: DSRed, first ~600 bp of the pDSRed2 coding region (Clontech); *eIF4G*, first ~650 bp of the coding region (Herold et al., 2001); *ofs*, HFA14207 (GenomeRNAi Database, www.dkfz.de/signaling2/rnai/); and *eIF4A* (*eIF-4A*), HFA03526. Target regions were amplified from cDNA using primers with 5′ T7 promoter sequences appended, and dsRNAs were synthesized (MEGAscript T7 kit. Ambion). dsRNA knockdown was performed as described (Clemens et al., 2000). Double knockdowns used twice as much total dsRNA.

Growth and rescue experiment overview: day 1, plated 4.5×10$^{6}$ cells per well and dsRNA treated; day 2, transfected as above; days 4 and 7, split cells 1:3; days 2, 3, 4, 6, 8 and 10, counted cells (hemacytometer). On day 8, cells were harvested, washed, fixed overnight in cold 70% ethanol and stained with propidium iodide solution. They were then sorted on a Becton-Dickinson FACSort machine running CellQuest Pro software. Cell cycle profiles were determined on FlowJo software using the Watson algorithm. All constructs used the Actin5C promoter, with eGFP kindly provided by Sara Cherry (University of Pennsylvania, Philadelphia, PA), and *GFP-ofs* and *GFP-eIF4G* both generated using the *Drosophila* Gateway system and the pENTR/D-TOPO kit (Invitrogen) (Huynh and Zieler, 1999).

### Western blotting

Each 1 ml of S2R+ cells from the growth experiment was lysed in 50 μl of 50 mM Tris (pH 7.5), 150 mM NaCl, 1% NP40, 10% glycerol, 1.5 mM EGTA on ice, combined with 2×SDS-PAGE sample buffer and boiled. Approximately 1-5 μl of lysate was loaded, adjusting for differences in cell numbers. Blots were blocked in 5% milk in TBS +0.1% Triton X-100, then cut to probe the same filter with experimental and loading control antibodies: 1:5000 mouse α-GFP (Clontech), 1:100,000 rabbit α-eIF4G (p180) (Zapata et al., 1994), 1:10,000 mouse α-alpha-tubulin (B512; Sigma), 1:5000 rabbit α-eIF4E (eIF-4E), 1:5000 mouse α-FLAG (F3165; Sigma), diluted in 2% milk (GFP antibody) or 5% milk (all others). HRP-coupled secondary antibodies (1:2000; Vector) were used for ECL detection (Amersham).

## RESULTS

### *off-schedule* is required for meiotic progression and spermatid differentiation

In wild-type flies, elongated sperm tails fill the majority of the testis tube. In the course of screening for defects in spermatogenesis, we noticed a severe reduction in sperm tails in the small deletion mutant 3572D-175ca (data not shown). Complementation analysis against EMS-induced male sterile mutants (Wakimoto et al., 2004) uncovered a second, stronger allele, Z3-3283, mutations in which produced no sperm tails (Fig. 1B). Z3-3283 testes were instead filled with cells resembling primary spermatocytes, having large nuclei and prominent nucleoli (Fig. 1D,E, red nuclei). In wild type, spermatid differentiation was first evident with the appearance of a spherical, phase-dark mitochondrial derivative (Fig. 1D, purple). In the mutants, mitochondria instead formed a dissociated mass next to

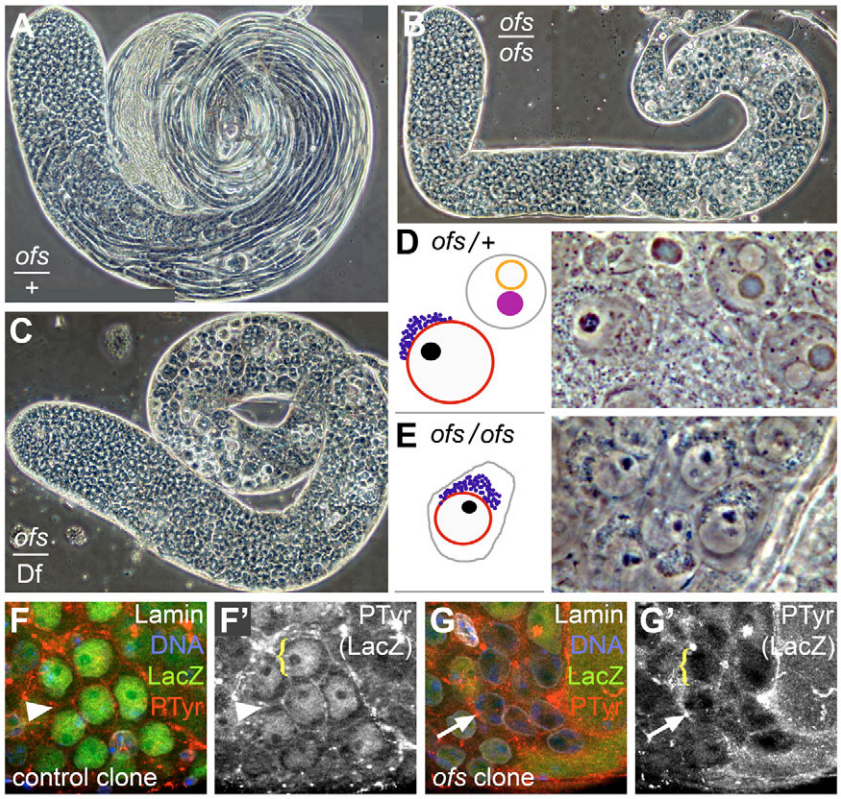


**Fig. 1. *ofs* mutants fail to undergo meiosis or differentiation.** (A-C) Phase images, apical-tip oriented to the left. (**A**) Heterozygous testes appear wild-type, with elongating spermatids filling most of the testis. (**B**) Mutant testes lack elongating spermatids. (**C**) *ofs*/Df(3R)*mbc*-R1 is indistinguishable from *ofs*/*ofs* (B). (**D**,**E**) High-magnification, with diagrams of the represented stages. Color code: primary spermatocyte nucleus, red; nucleolus, black; haploid spermatid nucleus, orange; fused mitochondrial derivative, purple; dissociated mitochondria, blue; cell outlines (where discernable), gray. (D) Heterozygous testes have examples of mature primary spermatocytes (left) and onion-stage spermatids (right). (E) The most prevalent cells found in *ofs* testes resemble primary spermatocytes. (**F**,**G**) Whole-mount immunofluorescent images of wild-type (F, arrowhead, 2×*lacZ*$^{+}$) and *ofs* (G, arrow, *lacZ*$^{-}$) clones in a heterozygous background. Flies were aged 4 days after clone induction, which allowed clones to progress midway through the meiotic $G_2$ of wild-type spermatocytes. (**F′**,**G′**) Brackets are the same size in each panel, highlighting the cell size difference between the two clones. The entire *ofs* cell outline (PTyr, phospho-Tyrosine) is approximately the same size as the nucleus of the control cell.

the nucleus (Fig. 1E, blue). These observations suggested that mutant spermatocytes did not execute the meiotic $G_2$-M transition or significant spermatid differentiation. The phenotype was recessive (Fig. 1A), and no stronger with Z3-3283 placed over a deficiency (Fig. 1C). Thus, the Z3-3283 allele was probably a strong hypomorph or null for the gene we tentatively called *off-schedule* (*ofs*), and was used for all subsequent analyses.

Mutant spermatocytes appeared smaller than wild type (Fig. 1D,E, compare red nuclei). To confirm this, we induced both homozygous-mutant and homozygous-wild-type clones in heterozygous testes, and compared the cross-sectional area of young spermatocytes of each genotype. Mutant cells were identified by the loss of a *lacZ*-expressing chromosome (*lacZ*$^{-}$), whereas homozygous wild-type cells were identified by higher *lacZ* expression (roughly 2× higher) compared with heterozygotes (homozygous wild-type cells were termed 2×*lacZ*$^{+}$). We outlined the cell periphery, revealed by anti-phospho-Tyrosine, and found that the cross-sectional area of *lacZ*$^{-}$ *ofs* cells was significantly smaller than age-matched 2×*lacZ*$^{+}$ wild-type cells induced in the same testis. For example, the mean±s.e.m. was 192±5.2 μm$^2$ versus 291±6.1 μm$^2$ ($n$=5 cells of each genotype; Student's $t$-test for matched pairs, $P$<0.001). Similar results were obtained in comparisons in two other testes. To rule out any contribution from second-site mutations, we also compared spermatocyte size in *ofs*/Df(3R)*mbc*-R1 testes versus heterozygous siblings. Young *ofs*/Df spermatocytes, defined as those first accumulating Boule protein (see below), were smaller than heterozygous sibling cells (mean±s.e.m.=314±15 μm$^2$ versus 448±14 μm$^2$, respectively; $n$=25 cells, five testes for each genotype; $P$=3.3×10$^{-8}$; see Fig. S1 in the supplementary material). Because decreased size could reflect a difference in ploidy, we assayed for pre-meiotic S phase in *ofs* mutants by BrdU incorporation. All germ cells within a cyst cycle synchronously, allowing us to distinguish pre-meiotic S phase from the mitotic S phases by counting the number of cells in each BrdU-positive (BrdU$^{+}$) cyst. The fraction of cysts per testis that were undergoing pre-meiotic S phase was similar in *ofs* compared to heterozygotes (0.4 versus 0.6, $n$=21 and 15 testes, respectively; $P$=0.42). Thus, the *ofs* spermatocytes progressed through pre-meiotic S phase normally, and were indeed in $G_2$ of their meiotic cell cycle. The smaller size of *ofs* spermatocytes must therefore reflect a defect in mass accumulation.

## *off-schedule* identifies a distinct pathway controlling spermatocyte development

The lack of meiosis and of any significant differentiation in *ofs* mutants was strongly reminiscent of the phenotype of spermatocyte-arrest mutants (Lin et al., 1996). *ofs* did not control Aly accumulation, which had the same spermatocyte nuclear localization in *ofs* mutants as in wild type (Fig. 2A,B, red). Furthermore, Cyclin A accumulation in *ofs* mutants revealed a phenotype distinct from that of the spermatocyte-arrest class. Normally, Cyclin A accumulated in the cytoplasm of $G_2$ spermatocytes (Fig. 2A, green). As spermatocytes near the $G_2$-M transition, Cyclin A translocates into the nucleus, where it is visible only briefly before it is degradation at metaphase (Eberhart et al., 1996; Lin et al., 1996). In spermatocyte-arrest mutants, Cyclin A accumulates normally, but then persists (Lin et al., 1996). By contrast, in *ofs* mutants, Cyclin A shifted to the nuclei of spermatocytes and was degraded (Fig. 2B, green, arrows; also see Fig. 3B, gold arrow). In addition, the timing of both nuclear translocation and eventual degradation dramatically differed from wild type. First, nuclear accumulation appeared more proximal to the testis tip than would normally occur (Fig. 2B). To establish whether this implied precocious movement of Cyclin A to the nucleus in mutant cells, we analyzed *ofs* mutant clones using cell position along the testis as a measure of developmental time.

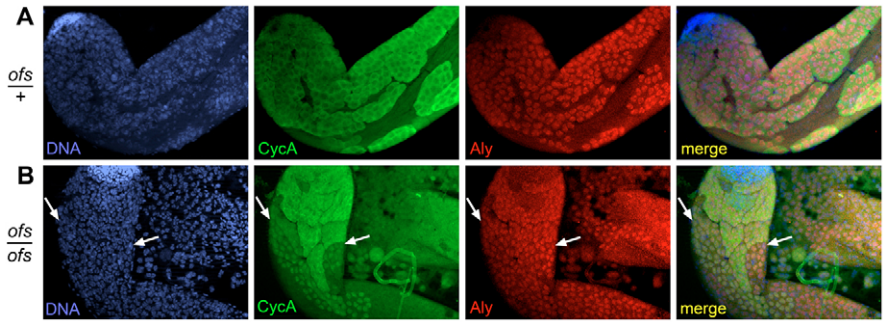


**Fig. 2. *ofs* identifies a distinct pathway controlling spermatocyte development.** (**A**,**B**) Immunofluorescent images of frozen split squashes. Aly staining (red) is indistinguishable between heterozygotes (A) and homozygotes (B). (A) Cyclin A (green) is predominantly cytoplasmic in heterozygous spermatocytes. (B) In the mutants, Cyclin A accumulates in nuclei (arrows) relatively close to the apical tip.

Indeed, Cyclin A was visible in the nucleus of mutant cells (Fig. 3A, arrows) that were much more proximally located relative to heterozygous cells, in which the translocation only occurred at meiosis I (Fig. 3A, arrowhead). Second, degradation of Cyclin A appeared delayed, because each *ofs* mutant testis had several cysts with nuclear Cyclin A, whereas there was, on average, less than one cyst in wild type (Fig. 2, green) (Lin et al., 1996). Mosaic analysis confirmed this, because Cyclin A persisted much longer in *ofs* mutant cells than in heterozygous control cysts (Fig. 3B, white arrows versus outline), although, eventually, it was degraded in mutant cells (Fig. 3B, gold arrow).

Whereas Cyclin A translocation was precocious, Boule accumulation was delayed. Boule is one target of the spermatocyte-arrest pathway and accumulates late in $G_2$ (Cheng et al., 1998; White-Cooper et al., 1998). In *ofs*/+ heterozygotes, germ cells approaching meiotic entry expressed both proteins (Fig. 3C, arrow). In *ofs* mutants, however, Cyclin A was degraded before Boule was first detected (Fig. 3D, line). Because Cyclin A persisted longer in *ofs* mutants, the fact that Cyclin A and Boule did not overlap suggested that the onset of Boule accumulation was significantly delayed. This was confirmed by scoring for Boule accumulation in homozygous mutant (*lacZ*$^{-}$ *ofs*) and homozygous wild-type (2×*lacZ*$^{+}$) clones at 2, 3, 6 and 8 days after clone induction. Whereas wild-type 2×*lacZ*$^{+}$ clones accumulated Boule by day 3, we did not detect Boule in *ofs* clones until day 6 (Table 1).

As a proposed translational regulator, Boule is necessary for the accumulation of Twine, the Cdc25 phosphatase that activates Cdc2 to initiate the $G_2$-M transition (Alphey et al., 1992). The delay in Boule accumulation should therefore cause a delay in Twine accumulation. Indeed, in *ofs* mutant testes, accumulation of a Twine translational reporter (White-Cooper et al., 1998) was observed in most mutant testes (15 out of 25), but at low levels and only in cells towards the base of the testis (Fig. 3F). Taken together, our data show that several key meiotic regulators exhibited advanced or delayed patterns in *ofs* mutants; hence the name *off-schedule*.

## *off-schedule* spermatocytes overexpress Roughex, which causes aberrant Cyclin A localization

The early cytoplasmic-to-nuclear shift of Cyclin A in *ofs* spermatocytes either reflected precocious execution of a normal event associated with the $G_2$-M transition or a different mechanism entirely. Normally, Cyclin A translocation is coincident with chromosomal condensation from a crescent-shaped to being more compact (Lin et al., 1996) (Fig. 3A, inset *ii*, lower cells). However, *ofs* mutant cells with nuclear Cyclin A exhibited chromosomal organization that more closely resembled early-stage heterozygous spermatocytes (Fig. 3A, insets). Therefore, the nuclear import of Cyclin A in *ofs* mutants was dissociated from other aspects of the $G_2$-M transition.

Similar precocious nuclear import had been observed upon overexpression of Roughex (Rux), a cyclin-dependent kinase inhibitor (Avedisov et al., 2000; Gönczy et al., 1994; Thomas et al., 1997). Indeed, we found that *ofs* mutant spermatocytes exhibited abnormal accumulation of Rux protein, and that Rux colocalized with nuclear Cyclin A (Fig. 4B, arrow). Furthermore, removal of *rux* activity prevented Cyclin A from accumulating in the nuclei of mutant spermatocytes (Fig. 4D, arrow). Thus, in *ofs* mutants, excess Rux accumulated, leading to aberrant, early nuclear Cyclin A localization (Fig. 4A). In contrast to this aberrant program, the normal cytoplasmic-to-nuclear transition of Cyclin A in wild-type cells was not associated with Rux accumulation, and still occurred when *rux* was absent (Fig. 4C). In summary, the changes in Cyclin A subcellular distribution observed in *ofs* mutants do not reflect precocious timing for the normal mechanism, but rather the engagement of a different mechanism entirely.

## Examining the block to meiosis in *off-schedule* spermatocytes

We considered whether the changes in protein accumulation that we observed for Cyclin A, Twine and Rux were sufficient to explain the block the $G_2$-M transition in *ofs* mutants. Because Twine accumulation was delayed in *ofs* mutants, we drove Twine accumulation in early spermatocytes using the transcriptional and translational regulatory sequences of β2-tubulin to try to rescue meiotic entry (Maines and Wasserman, 1999). However, the *ofs* mutant phenotype was not noticeably suppressed, even after also removing *rux* inhibition of Cyclin A/cyclin-dependent kinase (Cdk) activity (data not shown). This suggests that other effectors of the $G_2$-M transition are also affected in *ofs* mutants (perhaps Cyclin B, see Discussion).

## *off-schedule* encodes the predominant eIF4G-like protein in spermatocytes

To clone *ofs*, we defined the portion of the *ofs*$^{3572D\text{-}175ca}$ deletion crucial for its effects on spermatogenesis and identified a nonsense mutation in *ofs*$^{Z3\text{-}3283}$ (Fig. 5A; see Materials and methods). Both affected the CG10192 locus. We conducted transcript mapping, and assembled a full-length cDNA for transgenic rescue, using a promoter that expresses well in spermatocytes (see Materials and methods). *ofs* homozygotes inheriting the transgene were fully rescued to fertility (data not shown).

*ofs* encodes a 2072-residue protein with striking homology in the C terminus to the eukaryotic initiation factor 4 gamma (eIF4G). The N terminus did not exhibit any significant homology to other proteins. The bona fide eIF4G ortholog in *D. melanogaster* is CG10811 (also known as eIF-4G or eIF4G) (Hernandez et al., 1998; Zapata et al., 1994), which is 1666 amino acids in length and has

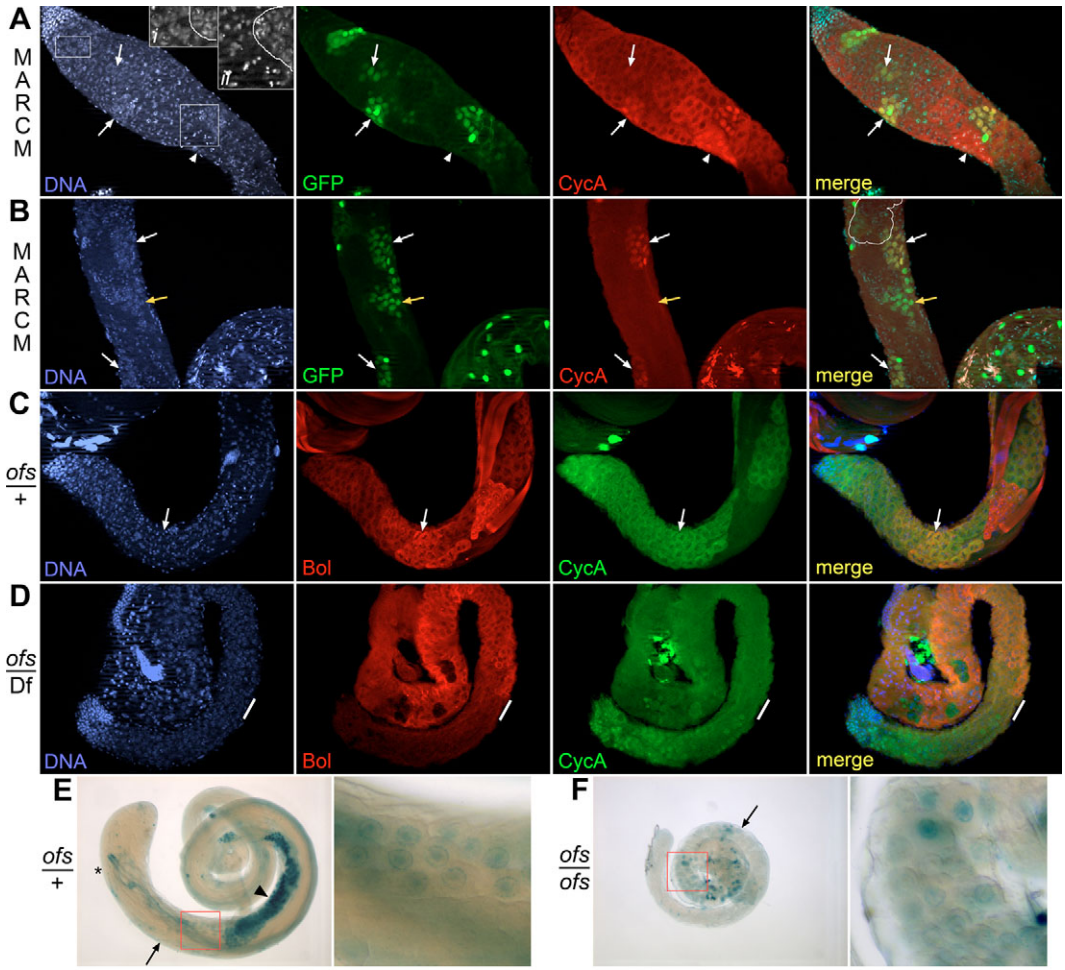


**Fig. 3. *ofs* mutants exhibit altered timing of Cyclin A, Boule and Twine accumulation.** (A-D) Whole-mount immunofluorescence. (A,B) *ofs* clones (GFP+, green) in a heterozygous background. (**A**) *ofs* clones precociously exhibit nuclear Cyclin A (CycA, arrows, red), whereas heterozygous spermatocytes are only beginning to accumulate Cyclin A, and nuclear entry occurs only in cysts entering the $G_2$-M transition (arrowhead). (Inset *i*) In early spermatocytes, the degree of chromatin condensation in *ofs* clones (outlined, upper right) is similar to heterozygous cells (left). (Inset *ii*) By contrast, older mutant cysts retain less condensed chromatin (outlined, upper right), whereas heterozygotes begin to condense chromatin as they approach meiosis (left-most and lower cells). (**B**) Midsection of the testis (tip is up) showing persistence of nuclear Cyclin A in clones (white arrows) past the meiotic region and its eventual degradation (yellow arrow). The position of the most advanced Cyclin A-containing heterozygous spermatocytes (located in a different focal plane) is outlined (merged panel). (**C**,**D**) In contrast to heterozygotes (C, arrow), in *ofs*/Df(3R)*mbc*-R1 mutants, Cyclin A (green) does not overlap with Boule (red) expression (D, line). Notice that *ofs*/Df has a slightly different (perhaps stronger) Cyclin A phenotype in which all spermatocyte staining is nuclear. (E,F) *twine-lacZ* reporter, X-Gal activity staining. (**E**) In heterozygotes (boxed area magnified on right) expression first appears faintly in nuclei of mature primary spermatocytes (arrow), becomes stronger during the meiotic divisions and is strongest in spermatids (arrowhead). Asterisk labels nonspecific, endogenous enzymatic activity. (**F**) In *ofs* mutants, expression is first detected relatively more distal in the testis tube (arrow) and resembles the mature primary spermatocyte signal.

higher overall similarity to eIF4G proteins from other species than does Ofs (Fig. 5B). Ofs and the *Drosophila* eIF4G protein have strong conservation in their C termini. The premature stop in $ofs^{Z3\text{-}3283}$ is upstream of the conserved regions, consistent with its strong loss-of-function phenotype.

*ofs* mRNA accumulates in spermatocytes and at post-meiotic stages (Fig. 5A,C). By contrast, *eIF4G* showed variable, low-level expression near the testis tip and less signal thereafter (Fig. 5D). eIF4G protein was detectable at low levels in early-stage germ cells, diminishing in spermatocytes, and at high levels in somatic tissues, such as the testis sheath (data not shown). Taken together with the cell size differences noted earlier, we propose that Ofs protein serves as the main eIF4G of the meiotic male germ line.

**Table 1. Boule accumulation is delayed in *ofs* mutant clones**

| Age of clones (days) | # testes with clones | ofs (*lacZ*⁻), # cysts | | Wild type (2×*lacZ*⁺), # cysts | |
|---|---|---|---|---|---|
| | | Bol⁺ | Bol⁻ | Bol⁺ | Bol⁻ |
| 2 | 5 | – | 7 | – | 2 |
| 3 | 9 | – | 17 | 4 | 9 |
| 6 | 9 | 2 | 32 | 13 | 18 |
| 8 | 1 | – | 3 | 2 | 2 |

Flies were aged for 2, 3, 6 and 8 days after clone induction. *ofs* clones lack the *lacZ* marker, whereas wild-type clones contain two copies of *lacZ*. Boule (Bol) accumulation was assessed by immunofluorescence. Both types of clones are equally as likely to be induced. The observed difference in the number of *ofs* versus wild-type clones is probably a reflection of our ability to reliably detect two copies of *lacZ* versus the one copy in the background.

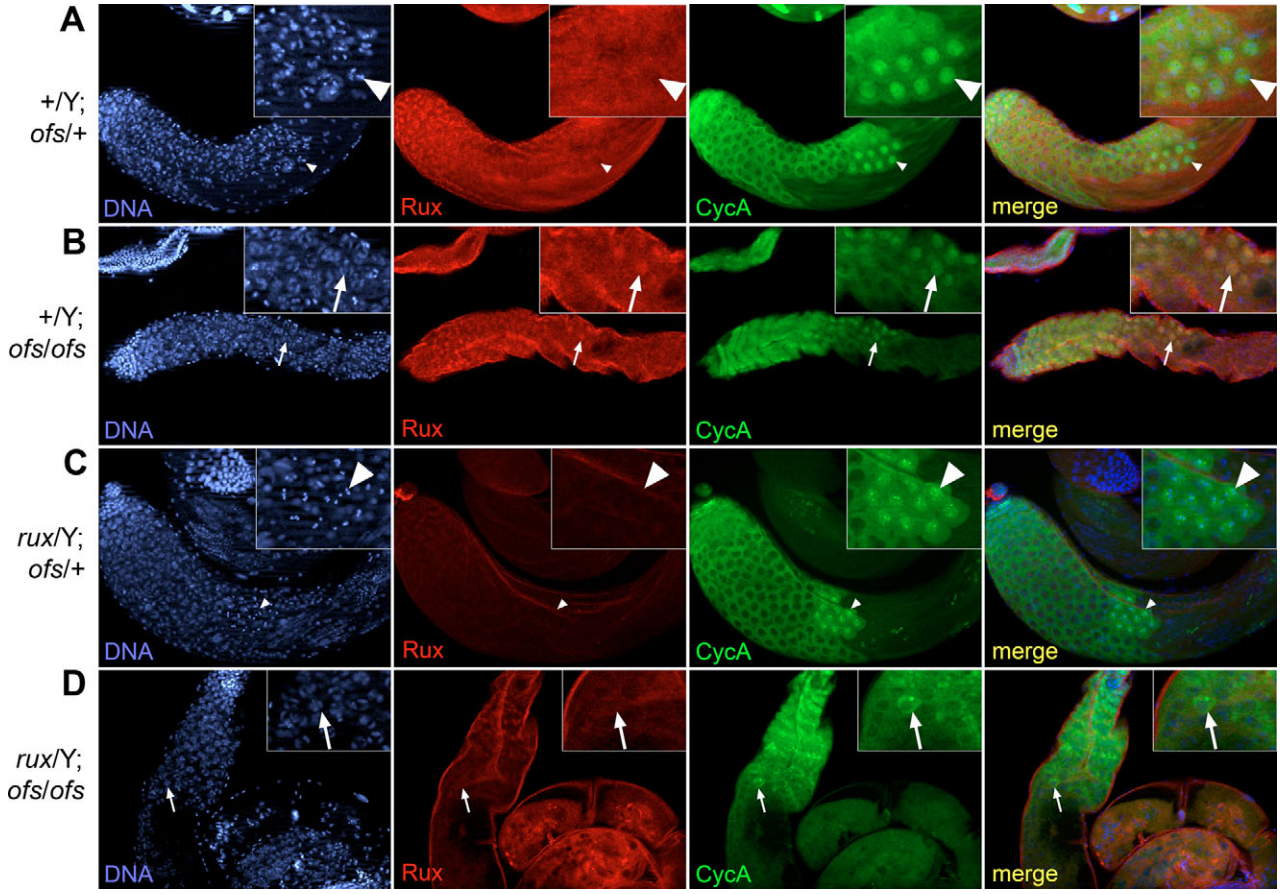


**Fig. 4. *ofs* spermatocytes activate an abnormal Cyclin A pattern due overexpression of Rux.** Whole-mount immunofluorescent images of siblings from a single cross. (**A**,**B**) $Rux^+$ progeny show nuclear Cyclin A (CycA, green) co-localized with Rux (red) accumulation in *ofs* mutants (B, arrow), but not in their heterozygous siblings (A, arrowhead). (**C**) Siblings heterozygous for *ofs* still show Cyclin A nuclear translocation in the absence of *rux* function (arrowhead). (**D**) *ofs* mutants inheriting the $rux^9$ mutation have only cytoplasmic localization of Cyclin A (arrow).

As such, Ofs should associate with mRNA cap complexes, as does canonical eIF4G, and should functionally substitute for eIF4G in cultured cells.

## Off-schedule is pulled down by 7-methyl-GTP Sepharose from S2R+ cell extracts

In cap-dependent translation, the eIF4F complex, made up of eIF4G, eIF4A and eIF4E, acts as a bridge between the mRNA cap and the 40S ribosomal subunit. eIF4E binds the modified cap structure of mature mRNAs, whereas eIF4A is an RNA helicase that unwinds secondary structure (Prevot et al., 2003). To establish whether Ofs could associate with mRNA caps, we incubated extracts of S2R+ cells expressing epitope-tagged versions of Ofs or eIF4G with 7-methyl-GTP Sepharose and identified bound proteins by SDS-PAGE western analysis. Both Ofs and eIF4G associated with 7-methyl-GTP Sepharose but not with control Sepharose beads (Fig. 6). Thus, by inference, Ofs can associate with mature mRNAs in cultured cells.

## Off-schedule has an eIF4G-like function in S2R+ cells

To address the ability of Ofs to functionally replace eIF4G, we depleted cultured cells of eIF4G or Ofs, singly and in combination, using double-stranded RNA (dsRNA). Depletion of eIF4G alone caused a statistically significant decrease in cell number (Fig. 7A, orange triangles). Although depletion of Ofs alone had no effect (Fig. 7A, green Xs), the combined depletion of Ofs and eIF4G exhibited a more dramatic effect than eIF4G alone, approaching the effect of eIF4A (also known as eIF-4A – FlyBase) knockdown (Fig. 7A, purple asterisks and gray circles). Thus, Ofs is partially redundant with eIF4G for S2R+ cell proliferation and/or viability. Western blots showed specific, extensive reduction in the levels of eIF4G and of transiently transfected GFP-Ofs by day 4 (Fig. 7B).

To examine what effect depletion of these proteins had on the cell cycle, we analyzed DNA content by FACS on day 8. A larger proportion of cells in the eIF4G alone and eIF4G+Ofs depletion conditions had $G_1$ DNA content, indicating that the $G_1$-S transition was delayed (Fig. 7D). This is consistent with the fact that the $G_1$-S transition is thought to be the major control point for growth sensing in mitotic cells of the fly (Stocker and Hafen, 2000). If a $G_1$ delay was the only effect, we would have expected to see a similar, compensatory decrease in both S and $G_2$. Instead, most of the decrease occurred in S phase. Thus, $G_2$ had also slowed, but to a lesser degree than $G_1$. Similar results have been reported previously (Bjorklund et al., 2006). As with the growth curves, the Ofs single depletion had no effect on the cell cycle profile.

We next assessed the ability of GFP-Ofs to rescue the growth defect. Cells were treated with dsRNA on day 1, transfected with a rescue construct on day 2, and GFP expressers (transfected) and

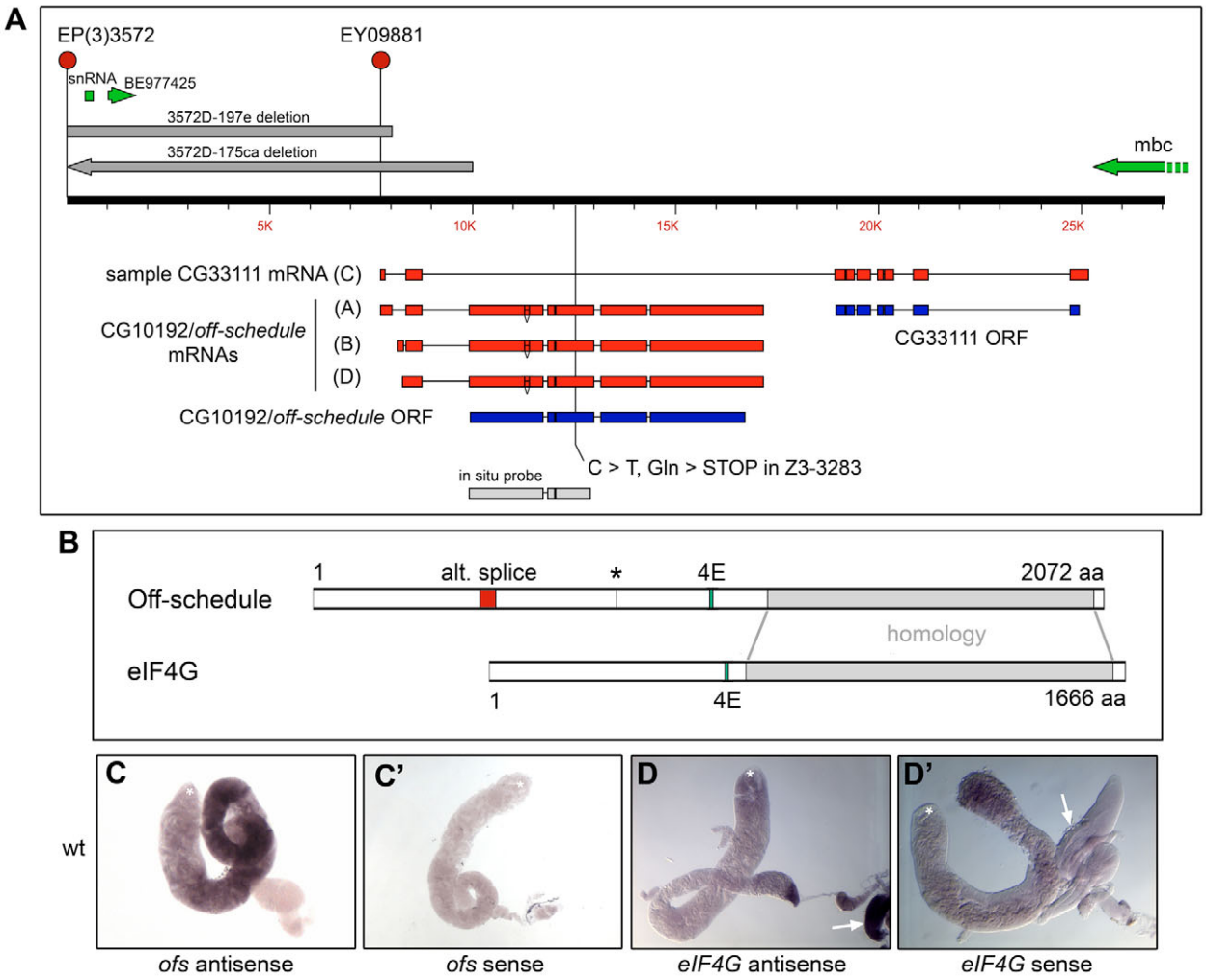


**Fig. 5. *ofs* encodes the main eIF4G in spermatocytes.** (**A**) Map of the genomic sequence of a portion of the right arm of Chromosome 3 indicating breakpoints of informative deletions (dark gray) and the Z3-3283 point mutation relative to transcripts (red, oriented 5′ to 3′) and coding regions (blue) for both CG10192 (*Ofs*) and CG33111. Also shown: in situ probes (light gray), insertion sites for nearby transposable elements (red circles) and flanking genes (green). (**B**) Predicted Ofs protein and *Drosophila* eIF4G. Locations are noted for the alternate splice (red), the premature stop in Z3-3283 (asterisk), predicted eIF4E-binding sites (green) and homologous regions (gray). Conserved domains are 27% identical and 43% similar, and include the predicted eIF4A-binding domains. (**C-D′**) In situ hybridizations to wild-type (wt) testes. Tips are marked with asterisks. (C) Antisense probe for *ofs* (see panel A) showed expression in spermatocytes. (D) Antisense probe to *eIF4G* showed low expression at the testis tip, and was undetectable thereafter. By contrast, somatic tissue stained strongly (arrows). (C′,D′) Sense probe controls.

non-expressers (untransfected) were counted for each well from days 3 through to 10. Whereas GFP alone could not rescue, cells expressing either GFP-Ofs or GFP-eIF4G now exhibited growth curves and cell cycle profiles indistinguishable from controls (Fig. 7C,E, respectively). Either protein rescued eIF4G deficiency with equal effectiveness. Because dsRNA treatment probably reduced the effectiveness of the cognate GFP-tagged protein (Fig. 7B), rescue was likely to be underestimated.

## DISCUSSION

Spermatocytes must execute meiosis and morphogenesis in the correct sequence to form functional sperm. In flies, many of the key genes necessary for this to occur are transcribed at once via activity of the spermatocyte-arrest genes. These transcripts are then regulated post-transcriptionally to ensure the proper timing of their target processes. The *ofs* mutant phenotype suggests that spermatocytes monitor growth during $G_2$ as one way to ensure that execution of the meiotic divisions is timed coordinately with spermatid differentiation.

### Off-schedule, translation initiation and growth control

Alignment among eIF4G sequences suggests that Ofs would be part of the eIF4F complex with eIF4A and eIF4E, and our demonstration of its association with 7-methyl GTP Sepharose strongly supports this. Although we did not test binding of Ofs directly to eIF4A, alignment of human and fly eIF4G proteins shows conservation of three out of four sets of amino acids necessary to bind eIF4A (Imataka and Sonenberg, 1997). Of 12 crucial residues, ten were identical in Ofs, one was a conservative (L>I) change, and the twelfth diverged in *Drosophila* eIF4G as well (data not shown). With regard to eIF4E binding, the putative binding site in Ofs has an

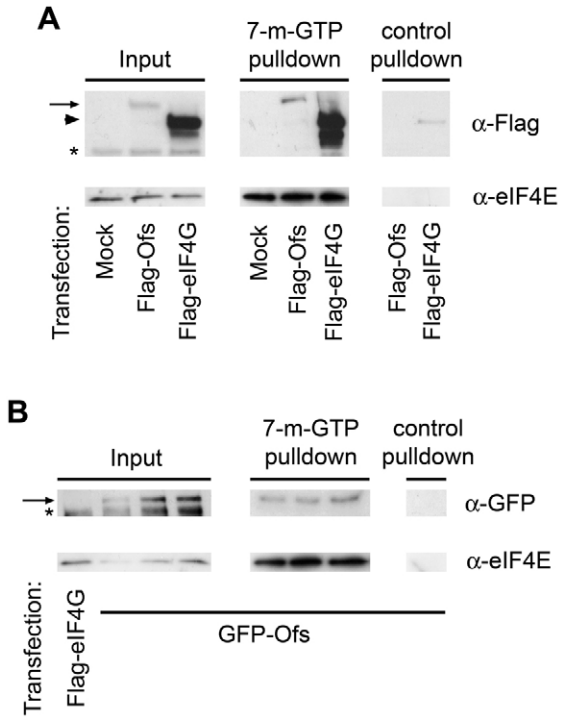


**Fig. 6. Ofs associates with an mRNA cap analog.** (**A,B**) Western blots of S2R+ cells transfected with Flag-Ofs or Flag-eIF4G (A) or with GFP-Ofs (B) and incubated with either 7-m-GTP-Sepharose (7-methyl-GTP Sepharose) beads or glutathione-Sepharose beads (control). Relevant bands are indicated with an arrow (Ofs constructs) or arrowhead (Flag-eIF4G). Asterisks indicate cross-reacting bands. Input lanes represent 2.5% of total lysate; pulldown lanes represent 100% of protein recovered from the beads. (A) Both Flag-Ofs and Flag-eIF4G are pulled down along with eIF4E by 7-m-GTP-Sepharose beads but not by control beads. (B) Binding is not due to the Flag epitope, because GFP-tagged Ofs also associated with 7-m-GTP-Sepharose beads. All conditions were repeated at least three times with comparable results.

arginine substituted for the usual hydrophobic residue (Mader et al., 1995). However, a similar substitution is tolerated in *Drosophila* eIF4E binding protein 1 (Miron et al., 2001), and Baker and Fuller present evidence for interaction with *Drosophila* eIF4E1 (Baker and Fuller, 2007). Taken together, it is quite likely that Ofs participates in cap-dependent translation initiation.

eIF4G (CG10811) and Ofs (CG10192) appear to be the only two eIF4G proteins encoded in the fly genome. One other candidate, l(2)01424, is more related to the proposed translational inhibitor, NAT1/p97 (Rpn1)/DAP5, than to eIF4G proteins (Takahashi et al., 2005). Although the novel N-terminus of Ofs raised the possibility that it would play a role distinct from eIF4G, our data suggest that Ofs can act as the only eIF4G in cultured cells. Whether these two proteins always act redundantly in vivo cannot be assessed without mutations in eIF4G. Nevertheless, eIF4G, at its endogenous level, cannot substitute for Ofs in spermatocytes. Perhaps this is simply due to a relatively lower level of eIF4G compared with Ofs. Alternatively, Ofs might uniquely aid in the translation of a special class of mRNAs, specific to spermatocyte development. Perhaps sequences in its novel N-terminus assist in such a role. Although further experiments are needed to distinguish between these possibilities, one reason for a distinction between spermatocytes and other cells might be in their respective mode of growth control.

In cultured eIF4G-deficient mitotic cells, the cell cycle effect we observed was on $G_1$, whereas the defect in spermatocyte progression was in $G_2$. Although the $G_1$-S transition is the major control point for growth sensing in mitotic cells of the fly (Stocker and Hafen, 2000), $G_2$ might make more sense as the control point for meiosis, because it is during this phase of the cycle that spermatocytes need to prepare not just for division, but for differentiation. Furthermore, spermatocytes might commit to the meiotic cycle, versus returning to the mitotic cycle, during $G_2$, as is the case for the yeast *Saccharomyces cerevisiae* (Simchen et al., 1972). Perhaps expressing a unique eIF4G (Ofs) in spermatocytes helps serve this role. Given the functional role for *ofs* as presented here and in the accompanying paper (Baker and Fuller, 2007), we propose that *ofs* henceforth be known as *eIF4G2* (also known as eIF-4G2 – FlyBase).

## Is sufficient growth during $G_2$ essential for meiotic progression?

Because *ofs* (*eIF4G2*) encodes the predominant eIF4G in spermatocytes, one might expect that mutant cells would exhibit decreased translation of many mRNAs. Just as we found a striking delay in Boule accumulation, other proteins would be expected to be similarly affected. Such a global deficit could account for the delayed development of these cells, and would be predicted to influence cell size, because the translational capacity of a cell predicts its ability to accumulate mass (Stocker and Hafen, 2000). Indeed, one of the earliest phenotypes in *eIF4G2* spermatocytes was their small size. Yet, we also found that Aly accumulation appeared normal and that Rux protein appeared to accumulate to an excess degree in early spermatocytes. These data demonstrate that some mRNAs are not affected by the translational deficit, and raise an alternative scenario wherein spermatocytes actively monitor their size. If they do not achieve proper growth, a checkpoint is induced to prohibit meiosis and differentiation. Because meiosis involves two cell divisions with little intervening interphase, size monitoring would be especially important before these cells commit to divide.

Circumstantial support for a growth checkpoint includes the accumulation of the Cdk inhibitor Rux, which leads to aberrant behavior of Cyclin A. In this model, the postulated checkpoint causes the striking delay in the accumulation of Boule, which, in turn, explains the delay in Twine accumulation. Eventually, Boule does accumulate to reasonable levels, perhaps as cells leak through the checkpoint, just as eventually occurs in mitotic checkpoints (Hartwell and Weinert, 1989). However, by then, Cyclin A has been degraded, and without it, the eventual accumulation of Twine cannot trigger meiosis, so the checkpoint has succeeded.

To establish that a checkpoint exists, one would need to identify the sensor, which detects the problem, and effectors, which execute inhibitory functions until the cell resolves the problem. We do not have a candidate for the sensor that detects growth at this time, nor for effectors controlling differentiation. However, we can speculate that Rux is one effector regulating the meiosis branch, where it could serve to inhibit Cyclin A-driven Cdc2 kinase activity (Avedisov et al., 2000). Rux is not the only effector regulating meiosis, however. Previous work showed that directly increasing the level of Rux only blocked entry into the second meiotic division (Gönczy et al., 1994). Consequently, the accumulation of Rux that we observe in *eIF4G2* mutants cannot fully explain the absence of the first meiotic division or the defect in differentiation. As would be typical for cell cycle regulation, several effectors must be activated at once to completely block the $G_2$-M transition.

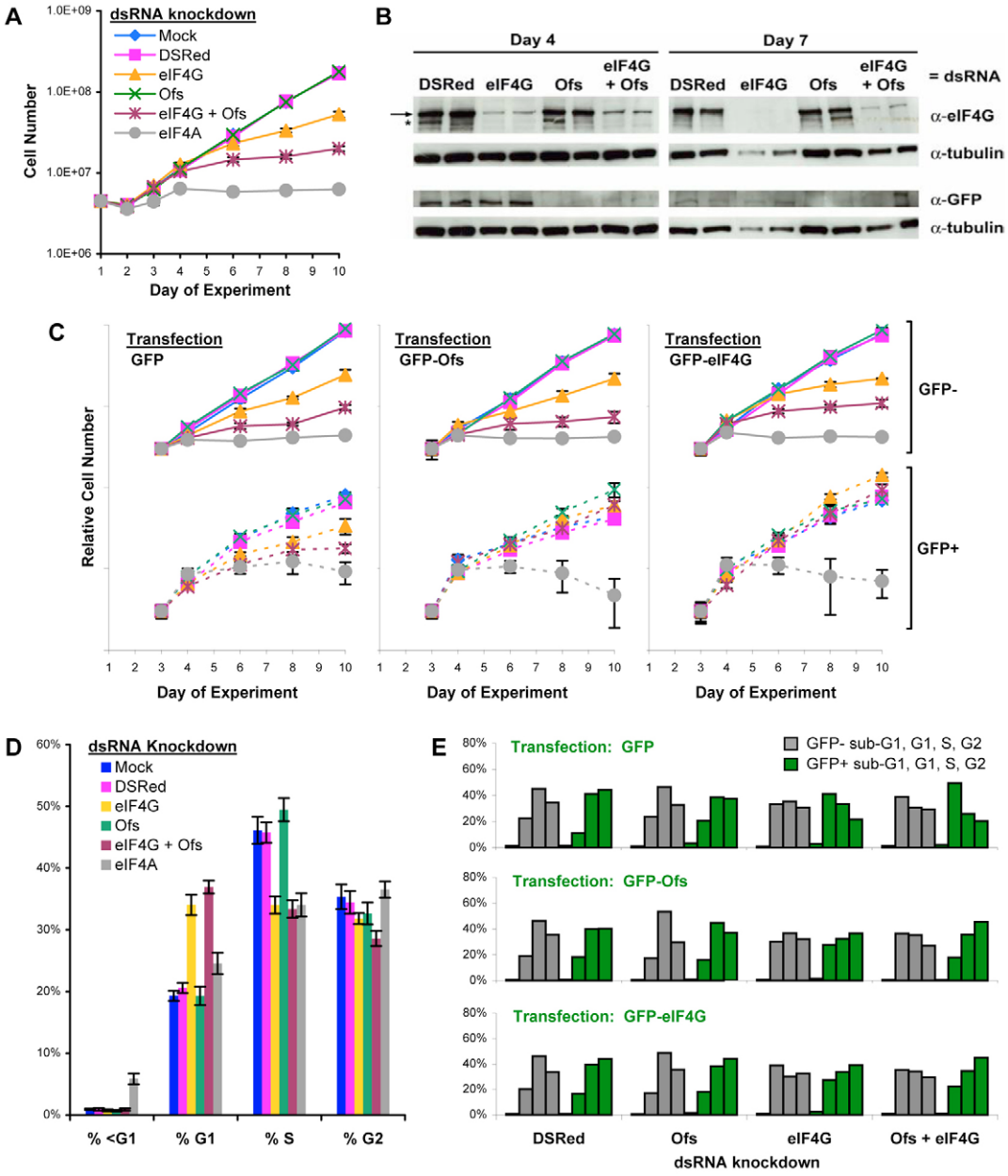


**Fig. 7. Ofs has an eIF4G-like function in S2R+ cells.** (**A**) Growth curves representing the average counts of GFP– (untransfected) cells from 10-13 wells with error bars representing s.e.m. (**B**) Western blot against eIF4G and GFP-Ofs assessing the degree of knockdown at days 4 and 7. The major eIF4G band is indicated with an arrow. We variably saw a second band migrating slightly faster (asterisk); its identity is unclear. (**C**) Matched growth curves for both GFP– (untransfected) and GFP+ (transfected) cells from wells transfected with GFP alone, GFP-Ofs or GFP-eIF4G. Curves were normalized for transfection efficiency at day 3. Key in A applies. Expression of GFP-Ofs or GFP-eIF4G completely rescues the defects caused by eIF4G or eIF4G+Ofs knockdown, but not by eIF4A knockdown. Each curve represents average counts from 3-6 wells, with error bars indicating s.e.m. (**D**) Cell cycle profiles for the cells represented in A showing a shift towards $G_1$ with either eIF4G or eIF4G+Ofs knockdown. eIF4A knockdown caused an increase in the percentage of cells with sub-$G_1$ DNA content, normally indicative of apoptotic cells (Oancea et al., 2006). (**E**) Summary of cell cycle profiling showing rescue by GFP-Ofs and GFP-eIF4G, but not by GFP alone. Gray bars (GFP–) and green bars (GFP+) are paired for each experimental condition. Within each set, from left to right: sub-$G_1$, $G_1$, S and $G_2$. Notice the relative shifts in the $G_1$ and $G_2$ bars: depletion of eIF4G-like proteins caused an increase in the proportion of $G_1$ cells (compare $G_1$ with $G_2$ bars), and this trend was reversed by transfection of either GFP-Ofs or GFP-eIF4G.

The existence of other effectors could explain why forcing early Twine accumulation failed to restore meiotic entry to *eIF4G2* mutants in a *rux* background. Alternatively, there might be additional positive factors necessary for $G_2$-M transition that have not accumulated in *eIF4G2* spermatocytes. Consistent with this, prior work driving expression of another Cdc25, *string* (*stg*), in early spermatocytes directed a normal rather than a precocious $G_2$-M transition (Sigrist et al., 1995). Thus, advancing Cdc25 activity is insufficient to trigger a precocious $G_2$-M even in the absence of a growth defect. Perhaps early spermatocytes have not had enough time to accumulate an essential component, such as Cyclin B, for the meiotic divisions. We found that *eIF4G2* mutant clones exhibited

Cyclin B levels comparable to neighboring heterozygous cells (data not shown). However, there is a peak in Cyclin B accumulation just prior to meiosis I (White-Cooper et al., 1998), and Baker and Fuller describe a deficit of this Cyclin B peak in *eIF4G2* mutants (Baker and Fuller, 2007). Thus, Cyclin B remains a candidate factor.

Whether a growth checkpoint exists or not, mass accumulation could be used to time the $G_2$-M transition by coupling rate-limiting cell cycle proteins to the translational capacity of the cell. In the budding yeast, *S. cerevisiae*, cyclin CLN3 (also known as YHC3) contains an upstream open reading frame in the 5′ UTR that slows its translation in $G_1$ under poor growth conditions (Polymenis and Schmidt, 1997). Similarly, during $G_2$ in the fission yeast, *Schizosaccharomyces pombe*, accumulation of CDC25 is disproportionately affected by defects in translation (Daga and Jimenez, 1999). Perhaps the translation of Boule, along with a few other meiotic cell cycle regulators, is disproportionately affected when translation is compromised in spermatocytes. Although this should be investigated, this simpler model does not explain the aberrant accumulation of Rux and the nuclear sequestration of Cyclin A that we observed.

## The role of growth control in spermatid differentiation

The defects in differentiation in *eIF4G2* mutants are not secondary to the meiotic block, because several cell cycle mutants fail to divide but still undergo substantial post-meiotic differentiation (Alphey et al., 1992; Eberhart et al., 1996; Eberhart and Wasserman, 1995; Sigrist et al., 1995). Several spermatid differentiation genes, such as *don juan* and *fuzzy onions*, are transcribed in primary spermatocytes under the control of spermatocyte arrest genes (White-Cooper et al., 1998). Translational control delays the accumulation of their protein products. This delay is functionally relevant, because precocious *don juan* accumulation leads to sterility (Hempel et al., 2006). In principle, then, the lack of significant differentiation in *eIF4G2* mutants could simply be due to a more pronounced translational delay for key differentiation genes. Alternatively, the block in differentiation might reflect a direct effect of the proposed growth checkpoint. Consistent with either model, the accumulation of the mitochondrial fusion protein Fuzzy onions is delayed, although we did not time this precisely (data not shown). We expect that other differentiation targets will also be abnormally delayed in *eIF4G2* mutants.

## Possible conservation of coupling translation initiation with meiotic progression

There are striking parallels to the role of eIF4G2 during spermatogenesis in other organisms. For instance, there are also two major isoforms of eIF4G in *Caenorhabditis elegans*, encoded by *ifg-1*. When the longest isoform was depleted from the germ line, oocytes arrested in meiosis I (B. D. Keiper, personal communication). The requirement for *ifg-1* in spermatogenesis has not yet been examined. However, one of the five isoforms of eIF4E in the worm, IFE-1, is clearly essential for spermatogenesis. RNA interference against *ife-1* results in delayed meiotic progression, and in defective sperm, in both hermaphrodites and males (Amiri et al., 2001). Furthermore, mouse testes carrying the Y chromosome deletion *Spy* (also known as *Eif2s3y* – Mouse Genome Informatics) have a meiotic arrest phenotype due to a lack of EIF2 (also known as EIF2S2 – Mouse Genome Informatics) function (Mazeyrat et al., 2001). Taken together, these examples suggest that translational control, and therefore possibly growth control, is a common theme for meiotic cycle cells.

We thank Jean Maines for unpublished work leading to our discovery of *ofs*; Catherine Baker, Minx Fuller and Brett Keiper for sharing unpublished data; Brooke Middlebrooks for generating transgenic fly lines; Paul Fisher, Ken Irvine, Gary Struhl, Julie Brill, Jamila Horabin, Jose Sierra, Helen White-Cooper, Barbara Thomas, Terence Murphy and Sara Cherry for essential reagents; Bruce Edgar for helpful insights on growth control; Edmund Koundakjian and Charles Zuker for their valuable mutant collection; Eric Sebzda for providing FACS expertise; and Colin Palmer, Tim Kelliher and Kate Rochlin for technical assistance. This work was funded by a NICHD grant T32HD07516 (T.M.F.-D.) and R01 grants from the NIH (GM60804, S.D. and HD60990, S.A.W.).

**Supplementary material**

Supplementary material for this article is available at
http://dev.biologists.org/cgi/content/full/134/15/2851/DC1

**References**

**Alphey, L., Jimenez, J., White-Cooper, H., Dawson, I., Nurse, P. and Glover, D. M.** (1992). twine, a cdc25 homolog that functions in the male and female germline of *Drosophila*. *Cell* **69**, 977-988.

**Amiri, A., Keiper, B. D., Kawasaki, I., Fan, Y., Kohara, Y., Rhoads, R. E. and Strome, S.** (2001). An isoform of eIF4E is a component of germ granules and is required for spermatogenesis in C. elegans. *Development* **128**, 3899-3912.

**Avedisov, S. N., Krasnoselskaya, I., Mortin, M. and Thomas, B. J.** (2000). Roughex mediates G(1) arrest through a physical association with cyclin A. *Mol. Cell. Biol.* **20**, 8220-8229.

**Ayyar, S., Jiang, J., Collu, A., White-Cooper, H. and White, R. A.** (2003). *Drosophila* TGIF is essential for developmentally regulated transcription in spermatogenesis. *Development* **130**, 2841-2852.

**Baker, C. C. and Fuller, M. T.** (2007). Translational control of meiotic cell cycle progression and spermatid differentiation in male germ cells by a novel eIF4G homolog. *Development* **134**, 2863-2869.

**Bjorklund, M., Taipale, M., Varjosalo, M., Saharinen, J., Lahdenpera, J. and Taipale, J.** (2006). Identification of pathways regulating cell size and cell-cycle progression by RNAi. *Nature* **439**, 1009-1013.

**Castrillon, D. H., Gönczy, P., Alexander, S., Rawson, R., Eberhart, C. G., Viswanathan, S., DiNardo, S. and Wasserman, S. A.** (1993). Toward a molecular genetic analysis of spermatogenesis in *Drosophila melanogaster*: Characterization of male-sterile mutants generated by single *P* element mutagenesis. *Genetics* **135**, 489-505.

**Cheng, M. H., Maines, J. Z. and Wasserman, S. A.** (1998). Biphasic subcellular localization of the DAZL-related protein boule in *Drosophila* spermatogenesis. *Dev. Biol.* **204**, 567-576.

**Clemens, J. C., Worby, C. A., Simonson-Leff, N., Muda, M., Maehama, T., Hemmings, B. A. and Dixon, J. E.** (2000). Use of double-stranded RNA interference in *Drosophila* cell lines to dissect signal transduction pathways. *Proc. Natl. Acad. Sci. USA* **97**, 6499-6503.

**Daga, R. R. and Jimenez, J.** (1999). Translational control of the cdc25 cell cycle phosphatase: a molecular mechanism coupling mitosis to cell growth. *J. Cell Sci.* **112**, 3137-3146.

**Eberhart, C. G. and Wasserman, S. A.** (1995). The pelota locus encodes a protein required for meiotic cell division: an analysis of G2/M arrest in *Drosophila* spermatogenesis. *Development* **121**, 3477-3486.

**Eberhart, C. G., Maines, J. Z. and Wasserman, S. A.** (1996). Meiotic cell cycle requirement for a fly homologue of human Deleted in Azoospermia [see comments]. *Nature* **381**, 783-785.

**Fuller, M. T.** (1993). Spermatogenesis. In *The Development of Drosophila melanogaster*. Vol. 1 (ed. M. Bate and A. Martinez-Arias), pp. 71-147. Cold Spring Harbor, NY: Cold Spring Harbor Laboratory Press.

**Gönczy, P., Viswanathan, S. and DiNardo, S.** (1992). Probing spermatogenesis in *Drosophila* with P-element enhancer detectors. *Development* **114**, 89-98.

**Gönczy, P., Thomas, B. J. and DiNardo, S.** (1994). roughex is a dose-dependent regulator of the second meiotic division during *Drosophila* spermatogenesis. *Cell* **77**, 1015-1025.

**Hales, K. G. and Fuller, M. T.** (1997). Developmentally regulated mitochondrial fusion mediated by a conserved, novel, predicted GTPase. *Cell* **90**, 121-129.

**Hartwell, L. H. and Weinert, T. A.** (1989). Checkpoints: controls that ensure the order of cell cycle events. *Science* **246**, 629-634.

**Hempel, L. U., Rathke, C., Raja, S. J. and Renkawitz-Pohl, R.** (2006). In *Drosophila*, don juan and don juan like encode proteins of the spermatid nucleus and the flagellum and both are regulated at the transcriptional level by the TAF II80 cannonball while translational repression is achieved by distinct elements. *Dev. Dyn.* **235**, 1053-1064.

**Hernandez, G., del Mar Castellano, M., Agudo, M. and Sierra, J. M.** (1998). Isolation and characterization of the cDNA and the gene for eukaryotic translation initiation factor 4G from *Drosophila* melanogaster. *Eur. J. Biochem.* **253**, 27-35.

**Herold, A., Klymenko, T. and Izaurralde, E.** (2001). NXF1/p15 heterodimers are essential for mRNA nuclear export in *Drosophila*. *RNA* **7**, 1768-1780.

**Hiller, M. A., Lin, T. Y., Wood, C. and Fuller, M. T.** (2001). Developmental

regulation of transcription by a tissue-specific TAF homolog. *Genes Dev.* **15**, 1021-1030.
**Hiller, M., Chen, X., Pringle, M. J., Suchorolski, M., Sancak, Y., Viswanathan, S., Bolival, B., Lin, T. Y., Marino, S. and Fuller, M. T.** (2004). Testis-specific TAF homologs collaborate to control a tissue-specific transcription program. *Development* **131**, 5297-5308.
**Horabin, J. I. and Schedl, P.** (1993). Sex-lethal autoregulation requires multiple cis-acting elements upstream and downstream of the male exon and appears to depend largely on controlling the use of the male exon 5′ splice site. *Mol. Cell. Biol.* **13**, 7734-7746.
**Huynh, C. Q. and Zieler, H.** (1999). Construction of modular and versatile plasmid vectors for the high-level expression of single or multiple genes in insects and insect cell lines. *J. Mol. Biol.* **288**, 13-20.
**Imataka, H. and Sonenberg, N.** (1997). Human eukaryotic translation initiation factor 4G (eIF4G) possesses two separate and independent binding sites for eIF4A. *Mol. Cell. Biol.* **17**, 6940-6947.
**Jiang, J. and White-Cooper, H.** (2003). Transcriptional activation in *Drosophila* spermatogenesis involves the mutually dependent function of aly and a novel meiotic arrest gene cookie monster. *Development* **130**, 563-573.
**Lee, T. and Luo, L.** (1999). Mosaic analysis with a repressible cell marker for studies of gene function in neuronal morphogenesis. *Neuron* **22**, 451-461.
**Li, M. G., Serr, M., Newman, E. A. and Hays, T. S.** (2004). The *Drosophila* tctex-1 light chain is dispensable for essential cytoplasmic dynein functions but is required during spermatid differentiation. *Mol. Biol. Cell* **15**, 3005-3014.
**Lin, T. Y., Viswanathan, S., Wood, C., Wilson, P. G., Wolf, N. and Fuller, M. T.** (1996). Coordinate developmental control of the meiotic cell cycle and spermatid differentiation in *Drosophila* males. *Development* **122**, 1331-1341.
**Mader, S., Lee, H., Pause, A. and Sonenberg, N.** (1995). The translation initiation factor eIF4E binds to a common motif shared by the translation factor eIF4 gamma and the translational repressors 4E-binding proteins. *Mol. Cell. Biol.* **15**, 4990-4997.
**Maines, J. Z. and Wasserman, S. A.** (1999). Post-transcriptional regulation of the meiotic Cdc25 protein Twine by the Dazl orthologue Boule. *Nat. Cell Biol.* **1**, 171-174.
**Mazeyrat, S., Saut, N., Grigoriev, V., Mahadevaiah, S. K., Ojarikre, O. A., Rattigan, A., Bishop, C., Eicher, E. M., Mitchell, M. J. and Burgoyne, P. S.** (2001). A Y-encoded subunit of the translation initiation factor Eif2 is essential for mouse spermatogenesis. *Nat. Genet.* **29**, 49-53.
**Miron, M., Verdu, J., Lachance, P. E., Birnbaum, M. J., Lasko, P. F. and Sonenberg, N.** (2001). The translational inhibitor 4E-BP is an effector of PI(3)K/Akt signalling and cell growth in *Drosophila*. *Nat. Cell Biol.* **3**, 596-601.
**Oancea, M., Mazumder, S., Crosby, M. E. and Almasan, A.** (2006). Apoptosis assays. *Methods Mol. Med.* **129**, 279-290.
**Olivieri, G. and Olivieri, A.** (1965). Autoradiographic study of nucleic acid synthesis during spermatogenesis in *Drosophila melanogaster*. *Mutat. Res.* **2**, 366-380.
**Perezgasga, L., Jiang, J., Bolival, B., Jr, Hiller, M., Benson, E., Fuller, M. T. and White-Cooper, H.** (2004). Regulation of transcription of meiotic cell cycle and terminal differentiation genes by the testis-specific Zn-finger protein matotopetli. *Development* **131**, 1691-1702.
**Polymenis, M. and Schmidt, E. V.** (1997). Coupling of cell division to cell growth by translational control of the G1 cyclin CLN3 in yeast. *Genes Dev.* **11**, 2522-2531.
**Preston, C. R. and Engels, W. R.** (1996). P-element-induced male recombination and gene conversion in *Drosophila*. *Genetics* **144**, 1611-1622.
**Prevot, D., Darlix, J. L. and Ohlmann, T.** (2003). Conducting the initiation of protein synthesis: the role of eIF4G. *Biol. Cell* **95**, 141-156.
**Rupes, I.** (2002). Checking cell size in yeast. *Trends Genet.* **18**, 479-485.
**Sigrist, S., Ried, G. and Lehner, C. F.** (1995). Dmcdc2 kinase is required for both meiotic divisions during *Drosophila* spermatogenesis and is activated by the Twine/cdc25 phosphatase. *Mech. Dev.* **53**, 247-260.
**Simchen, G., Pinon, R. and Salts, Y.** (1972). Sporulation in Saccharomyces cerevisiae: premeiotic DNA synthesis, readiness and commitment. *Exp. Cell Res.* **75**, 207-218.
**Smith, D. E. and Fisher, P. A.** (1989). Interconversion of *Drosophila* nuclear lamin isoforms during oogenesis, early embryogenesis, and upon entry of cultured cells into mitosis. *J. Cell Biol.* **108**, 255-265.
**Stocker, H. and Hafen, E.** (2000). Genetic control of cell size. *Curr. Opin. Genet. Dev.* **10**, 529-535.
**Takahashi, K., Maruyama, M., Tokuzawa, Y., Murakami, M., Oda, Y., Yoshikane, N., Makabe, K. W., Ichisaka, T. and Yamanaka, S.** (2005). Evolutionarily conserved non-AUG translation initiation in NAT1/p97/DAP5 (EIF4G2). *Genomics* **85**, 360-371.
**Terry, N. A., Tulina, N., Matunis, E. and DiNardo, S.** (2006). Novel regulators revealed by profiling *Drosophila* testis stem cells within their niche. *Dev. Biol.* **294**, 246-257.
**Thomas, B. J., Zavitz, K. H., Dong, X., Lane, M. E., Weigmann, K., Finley, R. L., Jr, Brent, R., Lehner, C. F. and Zipursky, S. L.** (1997). roughex down-regulates G2 cyclins in G1. *Genes Dev.* **11**, 1289-1298.
**Wakimoto, B. T., Lindsley, D. L. and Herrera, C.** (2004). Toward a comprehensive genetic analysis of male fertility in *Drosophila* melanogaster. *Genetics* **167**, 207-216.
**Wallenfang, M. R., Nayak, R. and DiNardo, S.** (2006). Dynamics of the male germline stem cell population during aging of *Drosophila* melanogaster. *Aging Cell* **5**, 297-304.
**White-Cooper, H., Schafer, M. A., Alphey, L. S. and Fuller, M. T.** (1998). Transcriptional and post-transcriptional control mechanisms coordinate the onset of spermatid differentiation with meiosis I in *Drosophila*. *Development* **125**, 125-134.
**White-Cooper, H., Leroy, D., MacQueen, A. and Fuller, M. T.** (2000). Transcription of meiotic cell cycle and terminal differentiation genes depends on a conserved chromatin associated protein, whose nuclear localisation is regulated. *Development* **127**, 5463-5473.
**Zapata, J. M., Martinez, M. A. and Sierra, J. M.** (1994). Purification and characterization of eukaryotic polypeptide chain initiation factor 4F from *Drosophila* melanogaster embryos. *J. Biol. Chem.* **269**, 18047-18052.